AIMS Mathematics, 9(4): 10031–10049.
DOI:10.3934/math.2024491
Received: 27 December 2023
Revised: 10 February 2024
Accepted: 19 February 2024
Published: 13 March 2024

http://www.aimspress.com/journal/Math

Research article

Neighbor event-triggered adaptive distributed control for multiagent systems with dead-zone inputs

Xiaohang Su, Peng Liu*, Haoran Jiang and Xinyu Yu

School of Automation, Guangdong University of Technology, Guangzhou 510006, China

* **Correspondence:** Email: liusir@outlook.com; Tel: +86-13424003557.

Abstract: The paper focused on the distributed tracking problem for a specific class of multi-agent systems, characterized by bandwidth constraint and dead zone actuators, where the bandwidth limitations exist in neighbor agents and the dead zone nonlinearity refers to a generalized mathematical model. Initially, a series of event-triggered mechanisms with relative thresholds were established for neighbor agents, ensuring that control signals were transmitted only when necessary. Next, the generalized dead zone models were decomposed into two parts: indefinite terms with control coefficients and disturbance-like terms, resulting in unpredictability and damaging effects. Subsequently, based on the backstepping procedure, final consensus controllers with multiple polynomial compensators were constructed. These controllers offset the coupling coefficients caused by event-triggered mechanisms and dead zone non-smooth. Stability analysis was given to substantiate the theoretical correctness of this method and support the claim of Zeno behavior avoidance. Finally, simulation studies were performed for the feasibility of our proposed methodology.

Keywords: multiagent systems; dead zone; event-triggered; adaptive control; distributed control
Mathematics Subject Classification: 93B52, 93C95, 93D05

1. Introduction

The event-triggered approach has attracted considerable attention because it provides an alternative solution for updates or operations based on specific events or conditions, rather than relying on fixed time intervals. Originally, the event-triggered strategy was regarded as an optimal control problem [1], and there were studies investigating the input constraints problem of unknown nonlinear systems [2] or switched nonlinear systems [3]. These investigated problems involve the implementation of a nominal system and a discounted cost function, but ignore how to guarantee system performance simultaneously. In recent years, event triggering has emerged as a pivotal concept in the realm of control systems. The fundamental idea behind control system based on event triggering was to update

control input only when specific triggering conditions were met, thereby optimizing the use of system resources [4]. The result performed how to keep balance between communication wastage and system performance, and this index has been noticed by more researchers [5]. For example, an adaptive neural network control scheme based on event-triggering [6] was developed for nonlinear systems characterized by sensor faults, input saturation, unknown control directions, and external disturbances. The study [7] proposed a method to set up periodically updated event-triggered conditions, leading the controller and parameter estimator to trigger events simultaneously. This research assures the asymptotic convergence of the calming error, effectively avoiding Zeno behavior. Separately, another study [8] introduced an adaptive event-triggered tracking approach based on a backstepping algorithm for a class of non-strict feedback nonlinear systems. This method combined intelligent technology for modeling unknown nonlinearities, and the event-triggering mechanism conserved communication resources through the transmission of discrete signals. Particularly, the results are further expanded to deal with multi-agent systems carrying with triggering control input [9]. For the multi-agent system with directed graphs, the research [10] introduced a new adaptive event-based protocol to tackle the consensus problem in linear quality. Furthermore, a novel dynamic control approach based on event triggering was introduced to address the consensus problem [11]. Further research [12] designed a new event-triggering mechanism suitable for the leader and an asynchronous edge event-triggering mechanism applicable to all edges. Combining with backstepping techniques, another article [13] proposed an adaptive scheme for fuzzy-based event-triggered containment control. The mentioned scheme is designed to update conditionally at specific sampling times for random nonlinear multi-agent systems with unidentified Bouc-Wen hysteresis inputs. All the approaches aim at conserving limited resources and reducing communication burdens. However, it is worth noting that nearly all the results have not accounted for bandwidth constraints associated with signal transmission between neighbor agents, let alone consider non-smooth actuator constraints additionally.

In the study of multi-agent systems, nonlinearities emerge as pivotal elements that profoundly influence system performance. Particularly, the occurrence of actuator dead zones are a pretty common phenomenon that cannot be overlooked. A dead zone is delineated by a specific region of input signal values where the actuator's output response is either zero or approaches zero. This phenomenon can lead to instability in the system, reducing control precision and production efficiency [14–17]. Therefore, research on actuator dead zones is essential for ensuring the stable operation and high performance of multi-agent systems. Some compensated methods have been used in the fields of industrial application. For example, the result in [18] proposed a new adaptive Fault Tolerant Control (FTC) method, in which the adaptive law estimated the effective gain and dead zone breakpoint of the actuator, effectively solving the dead zone phenomena in the robotic manipulator. Besides, the authors designed a compensator to mitigate the detrimental effects of dead zones on the control signal, successfully transforming the dead zone function into a linear form [19]. Additionally, another approach [20] proposed an innovative adaptive active FTC scheme specifically for wheeled robot systems. This scheme effectively compensated for actuator faults and dead zones, significantly enhancing the system's resistance to stability threats caused by dead zone phenomena. A novel distributed control strategy was advanced to effectively resolve complex game problems in the presence of actuator dead zones [21]. For intelligent control purpose, a fuzzy logic-based compensation method in [22] was set out to overcome the nonlinear challenges of actuator dead zones. This strategy avoids reliance on traditional dead zone inverse functions, instead using fuzzy rules to introduce offsets into

the control input. The fuzzy-based scheme was further applied to handle the problem posed by input dead zones in nonlinear systems [23], or addressed the nonlinear estimation and compensation issues caused by quantization and dead zones [24]. Another intelligent approach, named the Radial Basis Function Neural Networks, was utilized in [25], where an adaptive consistency control strategy was introduced, accomplishing comprehensive compensation for both input dead zones and actuator faults. Actually, the challenges posed by dead zone nonlinearites and network communication resources have been investigated in [26]. This study proposed an efficient designated tracking performance control method for Steer-by-Wire systems. This method not only compensates for the impacts of actuator faults and dead zones, but also achieves resource savings in network communication between actuators. However, despite the insights gained from the review of the aforementioned references, it is observed that there is a notable absence of research that concurrently considers dead zone phenomena of non-smooth actuators and neighbor communication constraints for multi-agent systems.

To fill this gap, this paper concentrates on the distributed control problem for multi-agent systems, taking into account the constraints on neighbor communication bandwidth and generalized dead zone inputs. The main contributions of this study are outlined as follows.

1. The existing literature has scarcely addressed the constraints imposed on neighbor communication bandwidth in multi-agent systems. In this context, we propose a more nuanced approach to construct neighbor event-triggered mechanisms, which feature a more adaptable structure for relative thresholds.

2. A novel compensatory strategy is presented to address the coupling model posed by generalized dead zone inputs and event-triggered coefficients. Moreover, the potential Zeno behavior can be avoided.

3. The majority of studies focus on event-triggered strategies to make the sacrifice of system performance achieve higher communication rates, but in this paper, stable performance in terms of consensus tracking errors are guaranteed to asymptotically converge to zero, while transient performance is also established.

The outline of this paper is as follows. Section 2 introduces the prerequisite knowledge and systems modeling. Controller designed procedure and stability analysis are given in section 3. Simulation study is shown to verify the effectiveness of the proposed method in section 4. Finally, section 5 gives a conclusion of this paper.

2. System modeling and background

2.1. Graph theory

By combining the principles of algebraic graph theory, we can abstract the communication networks of multi-agent systems. In this abstraction, the agents are represented as nodes, and the communication links are represented as edges. Depending on the nature of communication, the graph can be classified into different types. If the communication between any two nodes is mutual, it is referred to as a bidirectional graph. On the other hand, if the communication is unidirectional, the graph is called a directed graph, or simply an undirected graph. For a directed communication graph with M nodes, the set of all nodes is denoted as: $V = v_1, v_2, ..., v_M$. Each edge connecting two nodes v_i and v_j can be represented as $e_{i,j} = (v_i, v_j)$. The collection of all edges is denoted as E. If node v_i passes information to node v_j, we consider v_j as a neighbor of v_i. Additionally, there may be information incoming from

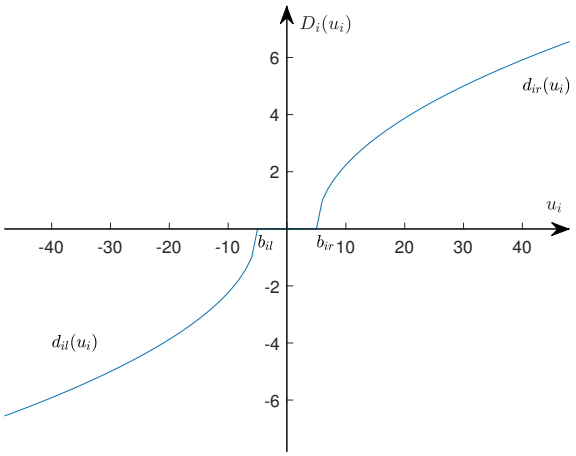

Figure 1. Dead zone model.

other nodes, forming the neighborhood set of v_i, which is also known as the in-degree of v_i. To account for the amplification or attenuation of information transmission, a weight coefficient a_{ij} is assigned to each edge. The weight coefficients of all edges form an adjacency matrix, where if $(v_i, v_j) \in E$, then $a_{ij} > 0$; otherwise, $a_{ij} = 0$ equals 0. A directed path from node i to node j is a sequence of nodes starting from i and ending at j such that each consecutive pair of nodes in the sequence corresponds to a directed edge in the graph.

2.2. *Multi-agents model*

In this study, we introduce a class of nonlinear multi-agent systems that are preceded by dead zone inputs.

$$\begin{aligned} \dot{x}_{i,j} &= x_{i,j+1} + \varphi_{i,j}^T(X_{i,j})\theta_i \\ \dot{x}_{i,n} &= \varphi_{i,0}(X_{i,n}) + \varphi_n^T(X_{i,n})\theta_i + D_i(u_i) \\ y_i &= x_{i,1} \end{aligned} \tag{2.1}$$

In this representation, the term $i = 1, 2, ..., m$ denotes the ith subagent, and $j = 1, 2, ..., n$ specifies the sequential order of each agent. The vector $X_{i,j} = [x_{i,1}, ..., x_{i,j}]^T$, which belongs to R^j, is defined as the variable vector, while the output of the ith agent is stated as y_i. The nonlinear functions $\varphi_{i,0}$ and $\varphi_{i,j}$ are known to be elements of R and R^n, respectively, and are characterized by their smoothness and continuity. Conversely, the parameter vector θ_i, also an element of R^n, remains unidentified and inaccessible. The input of the normal system corresponding to the ith subagent is signified by u_i, which is constrained by the dead zone nonlinearity expressed as $D_i(u_i)$. As illustrated in Figure 1, it is important to note that the model under examination includes mth dead zone models, and the dead zone constraints are encapsulated within a generalized structure detailed as follows:

$$D_i(u_i) = \begin{cases} \rho_{i,r}(t_{i,r})(u_i - b_{i,r}) & u_i \geq b_{i,r} \\ 0 & b_{i,l} < u_i < b_{i,r} \\ \rho_{i,l}(t_{i,l})(u_i - b_{i,l}) & u_i \leq b_{i,l} \end{cases} \tag{2.2}$$

Here, ρ_{i1} and ρ_{i2} represent bounded functions defined by the derivatives of the outputs of the ith dead zone model at specific instants, where $\rho_{i1} = \frac{\partial d_{i,r}(u_i)}{\partial u_i}\Big|_{u_i(t)=u_i(t_{i,r})}$ and $\rho_{i2} = \frac{\partial d_{i,l}(u_i)}{\partial u_i}\Big|_{u_i(t)=u_i(t_{i,l})}$. For the purpose of designing the controller, it is requisite to transform the dead zone model into a decomposed form:

$$D_i(u_i) = \rho_i(u_i)u_i + \epsilon_i(u_i) \tag{2.3}$$

where control coefficients are defined by $\rho_i(u_i)$ and bounded disturbance-like terms by $\epsilon_i(u_i)$ as indicated below:

$$\rho_i(u_i) = \begin{cases} \rho_{i,r}(t_{i,r}) & u_i \geq b_{i,r} \\ 0 & b_{i,l} < u_i < b_{i,r} \\ \rho_{i,l}(t_{i,l}) & u_i \leq b_{i,l} \end{cases} \tag{2.4}$$

$$\epsilon_i(u_i) = \begin{cases} -\rho_{i,r}(t_{i,r})b_{i,r} & u_i \geq b_{i,r} \\ 0 & b_{i,l} < u_i < b_{i,r} \\ -\rho_{i,l}(t_{i,l})b_{i,l} & u_i \leq b_{i,l} \end{cases} \tag{2.5}$$

for these two terms, which satisfy that

$$0 < \underline{\rho}_i \leq \rho_i(u_i) \leq \bar{\rho}_i < +\infty, \underline{\rho}_i = \min\{\rho_{i,r}, \rho_{i,l}\}, \bar{\rho}_i = \max\{\rho_{i,r}, \rho_{i,l}\} \tag{2.6}$$

$$|\epsilon_i(u_i)| \leq \max\{\rho_{i,r}b_{i,r}, -\rho_{i,l}b_{i,l}\} = \bar{\epsilon}_i \tag{2.7}$$

in which the limits are yet-undetermined positive constants. The control objectives of the present study are delineated as follows:

(a) The objective is to ensure that the outputs from all agents, denoted by y_i, can synchronously track the output signal of the leader, y_r.

(b) Another goal is to guarantee that all closed-loop signals remain cooperatively semi-globally uniformly ultimately bounded (CSUUB). In order to achieve these objectives, we establish the following assumptions:

Assumption 1. The information transmission graph G is fixed and connected. The output signal of the leader y_r is sufficiently smooth, bounded, and continuous, while its first nth derivative is available for its neighbor agents.

Assumption 2. The functions $d_{i,r}(u_i), d_{i,l}(u_i)$ are smooth, and there exist unknown positive constants $b_{i,r}, b_{i,l}$, such that $0 < \rho_{i,r}(t_{i,r}) < +\infty$, $\forall u_i \in [b_{i,r}, +\infty)$ and $0 < \rho_{i,l}(t_{i,l}) < +\infty$, $\forall u_i \in (-\infty, b_{i,l}]$.

2.3. Neighbor event-triggered mechanism

In the domain of event-triggered control, two predominant methodologies are employed for designing triggering mechanisms: the fixed threshold strategy and the relative threshold strategy.

The fixed threshold strategy is predicated on the establishment of a constant threshold. The criterion for event initiation is the attainment or breach of this threshold by the state change of the system under control. Typically, this threshold is predetermined and remains invariant to fluctuations in the state of the system. Nonetheless, this strategy may be susceptible to detection lapses and false alarms when processing voluminous datasets. Such pitfalls occur particularly when there are substantial shifts in data patterns, rendering the preset thresholds unsuitable and leading to erroneous triggerings.

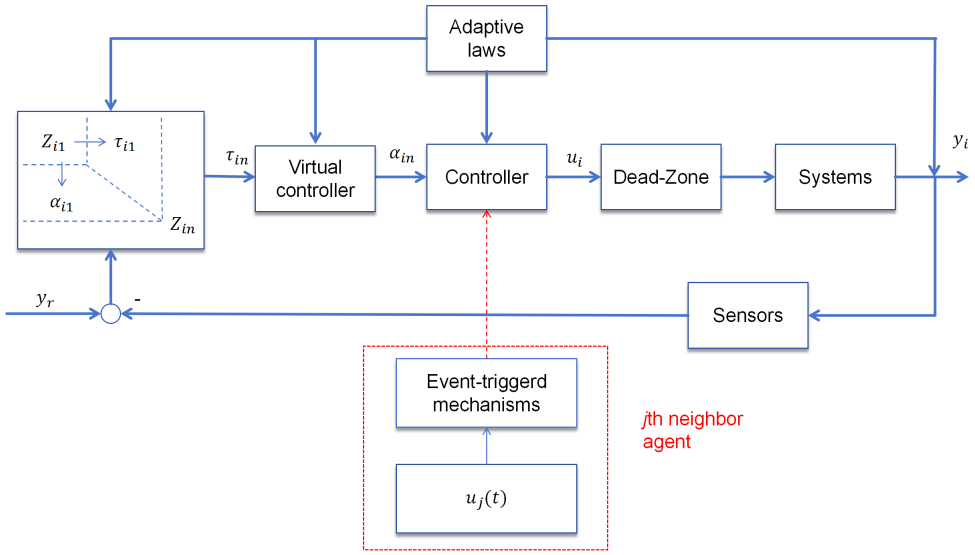

Figure 2. System model.

To mitigate these dilemmas, the relative threshold strategy is conceptualized. Distinct from its fixed counterpart, the relative threshold strategy adapts the triggering conditions dynamically in response to variations in the system state. Its core tenet is that if the system's state diverges from a set threshold by a specific margin for a given duration, an event trigger is deemed to have occurred, necessitating subsequent action. The usage of relative thresholds fortifies the system's stability and curtails superfluous energy expenditure and potential system volatility due to excessive event triggers.

Within the scope of this article, the relative threshold strategy is articulated through its application to inter-agent signal relay, particularly when the state variation surpasses a designated boundary. The neighbor control signal for the i^{th} agent from its j^{th} neighbor at time t is defined as $\breve{u}_j(t)$, which complies with the following equation:

$$\begin{aligned} &\breve{u}_j(t) = u_j(t) \\ &t_{k+1} = \inf\{t \in R||e_t(t)| \geq \delta|u_j(t)| + m_j\} \end{aligned} \tag{2.8}$$

where $0 < \delta < 1$ and $m_j > 0$ are predetermined constants. The term $e_t(t)$ represents the error threshold between $u_j(t)$ and $\breve{u}_j(t)$. When $e_t(t)$ surpasses the relative threshold as defined by $\delta|u_j(t)|+m$, the control signal $\breve{u}_j(t)$ is propagated to the neighboring agent.This nuanced approach is instrumental in achieving a balance between sensitivity and stability in event-triggered control systems.

Remark 1. Contrary to the existing literature by constructing event-triggered mechanisms for single agents, this paper works on solving the challenge of neighbor communication bandwidth constraints, and develops a more flexible relative threshold structure, where the system model is shown by Figure 2.

3. Distributed adaptive control design

In this section, we endeavor to amalgamate an event-triggering strategy with an adaptive control framework, refined by backstepping techniques, to fulfill our control objectives. The design process of the controller necessitates attention not only to the imperative of sustaining system stability but also to

the judicious use of bandwidth during communication between adjacent agents.

3.1. Controllers and adaptive laws design

The controller design unfolds through a recursive procedure, comprehensively described from step 1 through step n. As a preliminary to the design process, we introduce the definition of consensus errors. These errors will serve as pivotal variables in the development of our control laws and will inform the calculation of feedback signals necessary to drive the system toward the desired consensus state.

$$e_i = b_i(y_i - y_r) + \sum_{j=1}^{m} a_{i,j}(y_i - y_j) \tag{3.1}$$

where the connection coefficients b_i, d_i and $a_{i,j}$ are all known, and $j \in N_i$ represents the neighbor agent of the ith agent. The variables are further given as

$$\begin{aligned} z_{i,1} &= e_i, i = 1, 2, ..., m \\ z_{i,l} &= x_{i,l} - \alpha_{i,l-1}, l = 2, ..., n \end{aligned} \tag{3.2}$$

Step 1: Following (2.1), $\dot{z}_{i,1}$ is shown as

$$\begin{aligned} \dot{z}_{i,1} =& \dot{e}_i \\ =& (d_i + b_i)(z_{i,2} + \varphi_{i,1}^T\theta_i + \alpha_{i,1}) - \sum_{j=1}^{m} a_{i,j}\dot{x}_{j,1} - b_i\dot{y}_r \\ =& (d_i + b_i)(z_{i,2} + \varphi_{i,1}^T\theta_i + \alpha_{i,1}) - b_i\dot{y}_r - \sum_{j\in N_i} a_{i,j}x_{j,2} - \sum_{j\in N_i} a_{i,j}\varphi_{j,1}^T\theta_j \end{aligned} \tag{3.3}$$

where the first virtual controller $\alpha_{i,1}$ is set by

$$\alpha_{i,1} = \frac{1}{d_i + b_i}(-c_{i,1}z_{i,1} + b_i\dot{y}_r + \sum_{j\in N_i} a_{i,j}x_{j,2} + \sum_{j\in N_i} a_{i,j}\omega_{j,1}^T\hat{\theta}_j) - \omega_{i,1}^T\hat{\theta}_i \tag{3.4}$$

where $\omega_{i,1} = \varphi_{i,1}^T(X_{i,1})$ and $\omega_{j,1} = \varphi_{j,1}^T(X_{j,1})$. The including coefficient $c_{i,1}$ is a positive user-defined parameter, while $\hat{\theta}_i$ and $\hat{\theta}_j$ are the estimators of θ_i and θ_j, respectively.

Set a Lyapunov candidate as

$$V_{i,1} = \frac{1}{2}z_{i,1}^2 \tag{3.5}$$

whose derivative is computed as

$$\begin{aligned} \dot{V}_{i,1} =& z_{i,1}\Big((d_i + b_i)(z_{i,2} + \varphi_{i,1}^T\theta_i + \alpha_{i,1}) - b_i\dot{y}_r - \sum_{j\in N_i} a_{i,j}x_{j,2} - \sum_{j\in N_i} a_{i,j}\varphi_{j,1}^T\theta_j\Big) \\ =& (d_i + b_i)z_{i,1}z_{i,2} - c_{i,1}z_{i,1}^2 + (d_i + b_i)\tau_{i,1}\tilde{\theta}_i - \sum_{j\in N_i} a_{i,j}\tau_{j,1}^T\tilde{\theta}_j \end{aligned} \tag{3.6}$$

where the tuning functions $\tau_{i,1}$ and $\tau_{ij,1}$ are expressed by

$$\begin{aligned} \tau_{i,1} &= \omega_{i,1}z_{i,1} \\ \tau_{j,1} &= \omega_{j,1}z_{i,1} \end{aligned} \tag{3.7}$$

Step 2: From the definition of (2.1) and (3.3), $\dot{z}_2$ can be expressed as

$$\dot{z}_{i,2} = z_{i,3} + \alpha_{i,2} + \varphi_{i,2}^T\theta_i - \dot{\alpha}_{i,1} \tag{3.8}$$

where

$$\dot{\alpha}_{i,1} = \frac{\partial\alpha_{i,1}}{\partial x_{i,1}}(x_{i,2} + \varphi_{i,2}^T\theta_i) + \sum_{j=1}^{2}\frac{\partial\alpha_{i,1}}{\partial y_r^{(j-1)}}y_r^{(j)} + \frac{\partial\alpha_{i,1}}{\partial\hat{\theta}_i}\dot{\hat{\theta}}_i + \sum_{j\in N_i}\sum_{l=1}^{2}\frac{\partial\alpha_{i,1}}{\partial x_{j,l}}\dot{x}_{j,l} + \sum_{j\in N_i}\frac{\partial\alpha_{i,1}}{\partial\hat{\theta}_j}\dot{\hat{\theta}}_j \tag{3.9}$$

Set the virtual controller $\alpha_{i,2}$ by

$$\begin{aligned}\alpha_{i,2} =& -(d_i + b_i)z_{i,1} - c_{i,2}z_{i,2} - \omega_{i,2}\hat{\theta}_i + \frac{\partial\alpha_{i,1}}{\partial x_{i,1}}x_{i,2} + \sum_{j=1}^{2}\frac{\partial\alpha_{i,1}}{\partial y_r^{(j-1)}}y_r^{(j)}\\ &+ \sum_{j\in N_i}\sum_{l=1}^{2}\frac{\partial\alpha_{i,1}}{\partial x_{j,l}}x_{j,l+1} + \sum_{j\in N_i}\omega_{j,2}\hat{\theta}_j + \Gamma_1\frac{\partial\alpha_{i,1}}{\partial\hat{\theta}_i}\tau_{i,2} - \Gamma_2\sum_{j\in N_i}\frac{\partial\alpha_{j,1}}{\partial\hat{\theta}_j}\tau_{j,2}\end{aligned} \tag{3.10}$$

where Γ_1 and Γ_2 are user-defined symmetric positive matrices, and the tuning functions are given as

$$\begin{aligned}\tau_{i,2} &= (d_i + b_i)\tau_{i,1} + \omega_{i,2}z_{i,2}\\ \tau_{j,2} &= a_{i,j}\tau_{j,1} + \omega_{j,1}z_{i,1}\end{aligned} \tag{3.11}$$

accompanied by $\omega_{i,2} = \varphi_{i,2}^T - \frac{\partial\alpha_{i,1}}{\partial x_{i,1}}\varphi_{i,1}^T$ and $\omega_{j,2} = \sum\limits_{l=1}^{2}\frac{\partial\alpha_{i,1}}{\partial x_{j,l}}\varphi_{j,l}^T$.

Choose the Lyapunov candidate $V_{i,2}$ as

$$V_{i,2} = \frac{1}{2}\sum_{l=1}^{2}z_{i,l}^2 \tag{3.12}$$

With the previous definitions, one has

$$\begin{aligned}\dot{V}_{i,2} =&(d_i + b_i)z_{i,1}z_{i,2} - c_{i,1}z_{i,1}^2 + (d_i + b_i)\tau_{i,1}\tilde{\theta}_i - \sum_{j\in N_i}a_{i,j}\tau_{j,1}^T\tilde{\theta}_j + z_{i,2}\dot{z}_{i,2}\\ =& -\sum_{l=1}^{2}c_{i,l}z_{i,l}^2 + z_{i,2}z_{i,3} + [(d_i + b_i)\tau_{i,1} + \omega_{i,2}z_{i,2}]\tilde{\theta}_i + z_{i,2}\frac{\partial\alpha_{i,1}}{\partial\hat{\theta}_i}(\Gamma_1\tau_{i,2} - \dot{\hat{\theta}}_i)\\ &- \sum_{j\in N_i}[a_{i,j}\tau_{i,1} + \sum_{l=1}^{2}\frac{\partial\alpha_{i,1}}{\partial x_{i,l}}\varphi_{j,l}^T z_{i,1}]\tilde{\theta}_j - z_{i,2}\sum_{j\in N_i}\frac{\partial\alpha_{i,1}}{\partial\hat{\theta}_j}(\Gamma_2\tau_{j,2} + \dot{\hat{\theta}}_j)\\ =& -\sum_{l=1}^{2}c_{i,l}z_{i,l}^2 + z_{i,2}z_{i,3} + \tau_{i,2}\tilde{\theta}_i + z_{i,2}\frac{\partial\alpha_{i,1}}{\partial\hat{\theta}_i}(\Gamma_1\tau_{i,2} - \dot{\hat{\theta}}_i)\\ &- \sum_{j\in N_i}\tau_{j,2}\tilde{\theta}_j - z_{i,2}\sum_{j\in N_i}\frac{\partial\alpha_{i,1}}{\partial\hat{\theta}_j}(\Gamma_2\tau_{j,2} + \dot{\hat{\theta}}_j)\end{aligned} \tag{3.13}$$

Step l (l=3,...,n-1): The following steps can be summarized as

$$\dot{z}_{i,l} = z_{i,l+1} + \alpha_{i,l} + \varphi_{i,l}(X_{i,l})\theta_i - \dot{\alpha}_{i,l-1} \tag{3.14}$$

where

$$\begin{aligned}\dot{\alpha}_{i,l} = &\sum_{k=1}^{l-1}\frac{\partial\alpha_{i,l-1}}{\partial x_{i,k}}(x_{i,k+1}+\varphi_{i,k}^{T}\theta_i)+\sum_{k=1}^{l}\frac{\partial\alpha_{i,l-1}}{\partial y_r^{(k-1)}}y_r^{(k)}+\frac{\partial\alpha_{i,l-1}}{\partial\hat{\theta}_i}\dot{\hat{\theta}}_i+\sum_{j\in N_i}\frac{\partial\alpha_{i,l-1}}{\partial\hat{\theta}_j}\dot{\hat{\theta}}_j\\&+\sum_{j\in N_i}\sum_{k=1}^{l}\frac{\partial\alpha_{i,l-1}}{\partial x_{j,l}}\dot{x}_{j,l}\end{aligned}\tag{3.15}$$

The lth virtual controller is designed as

$$\begin{aligned}\alpha_{i,l} = &-c_{i,l}z_{i,l}-z_{i,l}-\omega_{i,l}\hat{\theta}_i+\sum_{k}^{l-1}\frac{\partial\alpha_{i,l-1}}{\partial x_{i,k}}x_{i,k+1}+\sum_{k=1}^{l}\frac{\partial\alpha_{i,l-1}}{\partial y_r^{(k-1)}}y_r^{(k)}\\&+\sum_{j\in N_i}\sum_{k=1}^{l}\frac{\partial\alpha_{i,l-1}}{\partial x_{j,k}}x_{j,k+1}+\sum_{j\in N_i}\omega_{j,l}\hat{\theta}_j+\Gamma_1\frac{\partial\alpha_{i,l-1}}{\partial\hat{\theta}_i}\tau_{i,l}-\Gamma_2\sum_{j\in N_i}\frac{\partial\alpha_{j,l-1}}{\partial\hat{\theta}_j}\tau_{j,l}\\&+\sum_{k=2}^{l-1}z_{i,k}\frac{\partial\alpha_{i,k-1}}{\partial\hat{\theta}_i}\Gamma_1\omega_{i,l}+\sum_{j\in N_i}\sum_{k=2}^{l-1}z_{i,k}\frac{\partial\alpha_{j,k-1}}{\partial\hat{\theta}_j}\Gamma_2\omega_{j,l}\end{aligned}\tag{3.16}$$

where

$$\begin{aligned}\tau_{i,l} &= \tau_{i,l-1}+\omega_{i,l}z_{i,l}\\ \tau_{j,l} &= \tau_{j,l-1}+\omega_{j,l}z_{i,l}\end{aligned}\tag{3.17}$$

with $\omega_{i,l} = \varphi_{i,l}^{T}-\sum\limits_{k=1}^{l-1}\frac{\partial\alpha_{i,l-1}}{\partial x_{i,k}}\varphi_{i,k}^{T}$ and $\omega_{j,l} = \sum\limits_{k=1}^{l}\frac{\partial\alpha_{i,l-1}}{\partial x_{j,k}}\varphi_{j,k}^{T}$.

The Lyapunov candidate is set as

$$V_{i,l} = \frac{1}{2}\sum_{k=1}^{l}z_{i,k}^{2}\tag{3.18}$$

then its derivative is expressed by

$$\begin{aligned}\dot{V}_{i,l} =&z_{i,l}\dot{z}_{i,l}+\dot{V}_{i,l-1}\\=&z_{i,l}(z_{i,l+1}+\alpha_{i,l}+\varphi_{i,l}\theta_i-\dot{\alpha}_{i,l-1})-\sum_{k=1}^{l-1}c_{i,k}z_{i,k}^{2}+z_{i,l-1}z_{i,l}+\tau_{i,l-1}\tilde{\theta}_i-\sum_{j\in N_i}\tau_{j,l-1}\tilde{\theta}_j\\&+\sum_{k=2}^{l-1}z_{i,k}\frac{\partial\alpha_{i,k-1}}{\partial\hat{\theta}_i}(\Gamma_1\tau_{i,l-1}-\dot{\hat{\theta}}_i)-\sum_{j\in N_i}\sum_{k=2}^{l-1}z_{i,k}\frac{\partial\alpha_{j,k-1}}{\partial\hat{\theta}_j}(\Gamma_2\tau_{j,l-1}+\dot{\hat{\theta}}_j)\\=&-\sum_{k=1}^{l}c_{i,k}z_{i,k}^{2}+z_{i,l}z_{i,l+1}+\tau_{i,l}\tilde{\theta}_i+\sum_{k=2}^{l}z_{i,k}\frac{\partial\alpha_{i,k-1}}{\partial\hat{\theta}_i}(\Gamma_1\tau_{i,l}-\dot{\hat{\theta}}_i)\\&-\sum_{j\in N_i}\tau_{j,l}\tilde{\theta}_j-\sum_{j\in N_i}\sum_{k=2}^{l}z_{i,k}\frac{\partial\alpha_{j,k-1}}{\partial\hat{\theta}_j}(\Gamma_2\tau_{j,l}+\dot{\hat{\theta}}_j)\end{aligned}\tag{3.19}$$

Step n: In this final step, the event-triggered mechanisms, consensus controllers and adaptive laws will be designed, respectively.

$$\begin{aligned}\dot{z}_{i,n} =&\varphi_{i,0} + \varphi_{i,n}\theta_i + D_i(u_i) - \dot{\alpha}_{i,n-1}\\ =&\varphi_{i,0} + \varphi_{i,n}\theta_i + D_i(u_i) - \sum_{k=1}^{n-1}\frac{\partial\alpha_{i,n-1}}{\partial x_{i,k}}(x_{i,k+1} + \varphi_{i,k}^T\theta_i) - \sum_{k=1}^{n}\frac{\partial\alpha_{i,n-1}}{\partial y_r^{(k-1)}}y_r^{(k)} - \frac{\partial\alpha_{i,n-1}}{\partial\hat{\theta}_i}\dot{\hat{\theta}}_i\\ &- \sum_{j\in N_i}\frac{\partial\alpha_{i,n-1}}{\partial\hat{\theta}_j}\dot{\hat{\theta}}_j - \sum_{j\in N_i}\sum_{k=1}^{n-1}\frac{\partial\alpha_{i,n-1}}{\partial x_{j,k}}\dot{x}_{j,k} - \sum_{j\in N_i}\frac{\partial\alpha_{i,n-1}}{\partial x_{j,n}}(\varphi_{j,0} + \varphi_{j,n}\theta_i + \breve{u}_j)\end{aligned} \tag{3.20}$$

The neighbor control signals $\breve{u}_j$ are transmitted if the designed events are triggered. As discussed in the result [27], $\breve{u}_j(t)$ is able to be rewritten as

$$\breve{u}_{j,k}(t) = \frac{u_{j,k}(t)}{1+\lambda_1(t)\delta} - \frac{\lambda_2(t)m_j}{1+\lambda_1(t)\delta} \tag{3.21}$$

where $\lambda_1(t), \lambda_2(t)$ are continuous parameters, satisfying $\lambda_{*k}(t) = 0, \lambda_{*k+1}(t) = \pm 1$ and $|\lambda_*(t)| \leq 1$, and $t_k(k \in Z^+)$ is the controller update time. The neighbor control signals contain the control coefficient terms and the unknown conventional constant terms. The virtual controller $\alpha_{i,n}$ is designed as

$$\begin{aligned}\alpha_{i,n} =& - c_{i,n}z_{i,n} - z_{i,n} - \omega_{i,n}\hat{\theta}_i + \sum_{k}^{n-1}\frac{\partial\alpha_{i,n-1}}{\partial x_{i,k}}x_{i,k+1} + \sum_{k=1}^{n}\frac{\partial\alpha_{i,n-1}}{\partial y_r^{(k-1)}}y_r^{(k)}\\ &+ \sum_{j\in N_i}\sum_{k=1}^{n-1}\frac{\partial\alpha_{i,n-1}}{\partial x_{j,k}}x_{j,k+1} + \sum_{j\in N_i}\omega_{j,n}\hat{\theta}_j + \frac{\partial\alpha_{i,n-1}}{\partial\hat{\theta}_i}\Gamma_1\tau_{i,n} - \sum_{j\in N_i}\frac{\partial\alpha_{j,n-1}}{\partial\hat{\theta}_j}\Gamma_2\tau_{j,n}\\ &+ \sum_{k=2}^{n-1}z_{i,k}\frac{\partial\alpha_{i,k-1}}{\partial\hat{\theta}_i}\Gamma_1\omega_{i,n} + \sum_{j\in N_i}\sum_{k=2}^{n-1}z_{i,k}\frac{\partial\alpha_{j,k-1}}{\partial\hat{\theta}_j}\Gamma_2\omega_{j,n}\end{aligned} \tag{3.22}$$

where

$$\begin{aligned}\tau_{i,n} &= \tau_{i,n-1} + \omega_{i,n}z_{i,n}\\ \tau_{j,n} &= \tau_{j,n-1} + \omega_{j,n}z_{i,n}\end{aligned} \tag{3.23}$$

with $\omega_{i,n} = \varphi_{i,n}^T - \sum_{k=1}^{n-1}\frac{\partial\alpha_{i,n-1}}{\partial x_{i,k}}\varphi_{i,k}^T$ and $\omega_{j,n} = \sum_{k=1}^{n}\frac{\partial\alpha_{i,n-1}}{\partial x_{j,k}}\varphi_{j,k}^T$.

The final controller u_i is designed as

$$u_i = \hat{\varrho}_i^T\nu_i \tag{3.24}$$

where $\hat{\varrho}_i = [\hat{\varrho}_{i1}, \hat{\varrho}_{i2}, \hat{\varrho}_{i3}, \hat{\varrho}_{i4}]^T$ is the estimate of $\varrho_i = [\frac{1}{\underline{\rho}_i}, \frac{\bar{\epsilon}_i}{\underline{\rho}_i}, \frac{1}{\underline{\rho}_i(1-\delta)}, \frac{1}{\underline{\rho}_i(1-\delta)}]^T$, accompanied by the update laws

$$\dot{\hat{\varrho}}_i = -\Gamma_\varrho\nu_i z_{i,n} \tag{3.25}$$

where Γ_ϱ is a user defined symmetric positive matrix. It is noted that $\dot{\hat{\varrho}}_i(t) \geq 0$ can be held. The term

$\nu_i = [\nu_{i1}, \nu_{i2}, \nu_{i3}, \nu_{i4}]^T$ is defined as

$$\begin{aligned}
\nu_{i1} &= -\frac{z_{i,n} q_{i1}^2}{\sqrt{z_{i,n}^2 q_{i1}^2 + \varepsilon_1(t)^2}}, q_{i1} = \varphi_{i,0} - \sum_{j \in N_i} \frac{\partial \alpha_{i,n-1}}{\partial x_{j,k}} \varphi_{j,0} - \alpha_{i,n} \\
\nu_{i2} &= -\frac{z_{i,n}}{\sqrt{z_{i,n}^2 + \varepsilon_2(t)^2}} \\
\nu_{i3} &= -\frac{z_{i,n} q_{i3}^2}{\sqrt{z_{i,n}^2 q_{i3}^2 + \varepsilon_3(t)^2}}, q_{i3} = -\sum_{j \in N_i} \frac{\partial \alpha_{i,n-1}}{\partial x_{j,n}} u_j \\
\nu_{i4} &= -\frac{z_{i,n} q_{i4}^2}{\sqrt{z_{i,n}^2 q_{i4}^2 + \varepsilon_4(t)^2}}, q_{i4} = \sum_{j \in N_i} \frac{\partial \alpha_{i,n-1}}{\partial x_{j,n}} m_j
\end{aligned} \tag{3.26}$$

It is worthy to point out that $z_{i,n} \hat{\varrho}_i^T \nu_i \leq 0$ can be always held if the initial values are chosen by $\hat{\varrho}_i(0) > 0$ for $i = 1, 2, 3, 4$. The update laws for $\hat{\theta}_i$ and $\hat{\theta}_j$ are given as

$$\dot{\hat{\theta}}_i = \Gamma_1 \tau_{i,n} \tag{3.27}$$

$$\dot{\hat{\theta}}_j = -\Gamma_2 \tau_{j,n}, j \in N_i \tag{3.28}$$

3.2. Stability analysis

Theorem 1. Consider the nonlinear MASs (2.1) with generated dead zone inputs (2.3), consisting of neighbor event-triggered mechanisms (2.8), consensus controllers (3.24) and adaptive update laws (3.27)–(3.28), under Assumptions 1–2. With any initial condition $V(0) < C$, the considered systems satisfy these characteristics:

a. All the closed-loop signals of the MASs are CSUUB.

b. The consensus errors asymptotically converge to zero.

c. Zeno behavior is able to be avoided.

Proof. Set the final Lyapunov function as

$$V = \sum_{i=1}^{m} (V_{i,n} + \frac{\rho_i}{2} \tilde{\varrho}_i^T \Gamma_\varrho^{-1} \tilde{\varrho}_i + \frac{1}{2} \tilde{\theta}_i^T \Gamma_1^{-1} \tilde{\theta}_i + \frac{1}{2} \sum_{j \in N_i} \tilde{\theta}_j^T \Gamma_2^{-1} \tilde{\theta}_j) \tag{3.29}$$

Via derivation operation, $\dot{V}_{i,n}$ can be expressed as

$$\begin{aligned}
\dot{V}_{i,n} =& z_{i,n}\dot{z}_{i,n} + \dot{V}_{i,n-1} \\
=& z_{i,n}(\varphi_{i,0} + \varphi_{i,n}\theta_i + D_i(u_i) - \dot{\alpha}_{i,n-1}) \\
& - \sum_{k=1}^{n-1} c_{i,k}z_{i,k}^2 + z_{i,n-1}z_{i,n} + \tau_{i,n-1}\tilde{\theta}_i - \sum_{j\in N_i}\tau_{j,n-1}\tilde{\theta}_j \\
& + \sum_{k=2}^{n-1} z_{i,k}\frac{\partial\alpha_{i,k-1}}{\partial\hat{\theta}_i}(\Gamma_1\tau_{i,n-1} - \dot{\hat{\theta}}_i) - \sum_{j\in N_i}\sum_{k=2}^{n-1} z_{i,k}\frac{\partial\alpha_{j,k-1}}{\partial\hat{\theta}_j}(\Gamma_2\tau_{j,n-1} + \dot{\hat{\theta}}_j) \\
=& z_{i,n}[q_{i1} + \rho_i(u_i)\hat{\underline{\varrho}}_i^T\nu_i + \epsilon_i(u_i) - \sum_{j\in N_i}\frac{\partial\alpha_{i,n-1}}{\partial x_{j,n}}\breve{u}_j] - \sum_{k=1}^{n} c_{i,k}z_{i,k}^2 + \tau_{i,n}\tilde{\theta}_i \\
& + \sum_{k=2}^{n} z_{i,k}\frac{\partial\alpha_{i,k-1}}{\partial\hat{\theta}_i}(\Gamma_1\tau_{i,n} - \dot{\hat{\theta}}_i) - \sum_{j\in N_i}\tau_{j,n}\tilde{\theta}_j - \sum_{j\in N_i}\sum_{k=2}^{n} z_{i,k}\frac{\partial\alpha_{j,k-1}}{\partial\hat{\theta}_j}(\Gamma_2\tau_{j,n} + \dot{\hat{\theta}}_j)
\end{aligned} \tag{3.30}$$

Applying (3.21) and (3.24) to the above equation, the including terms can be expressed as

$$\begin{aligned}
& z_{i,n}[q_{i1} + \rho_i(u_i)\hat{\underline{\varrho}}_i^T\nu_i + \epsilon_i(u_i) - \sum_{j\in N_i}\frac{\partial\alpha_{i,n-1}}{\partial x_{j,n}}\breve{u}_j] \\
=& z_{i,n}[q_{i1} + \rho_i\hat{\underline{\varrho}}_i^T\nu_i + \epsilon_i(u_i) - \sum_{j\in N_i}\frac{\partial\alpha_{i,n-1}}{\partial x_{j,n}}(\frac{u_j(t)}{1+\lambda_1(t)\delta} - \frac{\lambda_2(t)m_j}{1+\lambda_1(t)\delta})] \\
\leq& - z_{i,n}\underline{\rho}_i\tilde{\underline{\varrho}}_i^T\nu_i + z_{i,n}\underline{\rho}_i\underline{\varrho}_i^T\nu_i + |z_{i,n}q_{i1}| + \bar{\epsilon}_i|z_{i,n}| + \frac{1}{1-\delta}|z_{i,n}q_{i3}| + \frac{1}{1-\delta}|z_{i,n}q_{i4}| \\
=& - z_{i,n}\underline{\rho}_i\tilde{\underline{\varrho}}_i^T\nu_i + |z_{i,n}q_{i1}| - \frac{z_{i,n}^2q_{i1}^2}{\sqrt{z_{i,n}^2q_{i1}^2 + \varepsilon_1^2}} + \bar{\epsilon}_i(|z_{i,n}| - \frac{z_{i,n}^2}{\sqrt{z_{i,n}^2 + \varepsilon_2^2}}) \\
& + \frac{1}{1-\delta}(|z_{i,n}q_{i3}| - \frac{z_{i,n}^2q_{i3}^2}{\sqrt{z_{i,n}^2q_{i3}^2 + \varepsilon_3^2}}) + \frac{1}{1-\delta}(|z_{i,n}q_{i4}| - \frac{z_{i,n}^2q_{i4}^2}{\sqrt{z_{i,n}^2q_{i4}^2 + \varepsilon_4^2}})
\end{aligned} \tag{3.31}$$

Remark 2. As shown in Eq (3.31), the coupling model, which emerges from neighbor event-triggered mechanisms combined with decomposition dead zone models, can be classified into three components: the control coefficients term, the bounded disturbance-like term and the neighbor control signal term. To effectively handle this coupling model, the controller design necessitates the incorporation of multiple polynomial compensators, i.e., $u_i = \hat{\underline{\varrho}}_{i1}\nu_{i1} + \hat{\underline{\varrho}}_{i2}\nu_{i2} + \hat{\underline{\varrho}}_{i3}\nu_{i3} + \hat{\underline{\varrho}}_{i4}\nu_{i4}$.

With the property of $0 \leq |z| - \frac{z^2}{\sqrt{z^2+\varepsilon^2}} \leq \varepsilon$, $\dot{V}_{i,n}$ is rewritten by

$$\begin{aligned}
\dot{V}_{i,n} \leq& - z_{i,n}\underline{\rho}_i\tilde{\underline{\varrho}}_i^T\nu_i + \varepsilon_1 + \bar{\epsilon}_i\varepsilon_2 + \frac{\varepsilon_3}{1-\delta} + \frac{\varepsilon_4}{1-\delta} - \sum_{k=1}^{n} c_{i,k}z_{i,k}^2 + \tilde{\theta}_i\tau_{i,n} \\
& + \sum_{k=2}^{n} z_{i,k}\frac{\partial\alpha_{i,k-1}}{\partial\hat{\theta}_i}(\Gamma_1\tau_{i,n} - \dot{\hat{\theta}}_i) - \sum_{j\in N_i}\tilde{\theta}_j\tau_{j,n} - \sum_{j\in N_i}\sum_{k=2}^{n} z_{i,k}\frac{\partial\alpha_{j,k-1}}{\partial\hat{\theta}_j}(\Gamma_2\tau_{j,n} + \dot{\hat{\theta}}_j)
\end{aligned} \tag{3.32}$$

With the aid of update laws in (3.27)–(3.28), the derivative of final Lyapunov function V is expressed by

$$\begin{aligned}\dot{V} \leq & \sum_{i=1}^{m}[-\sum_{k=1}^{n} c_{i,k}z_{i,k}^2 - \Gamma_{\varrho}^{-1}\underline{\rho}_i\tilde{\varrho}_i^T(\Gamma_{\varrho}\nu_i z_{i,n} + \dot{\hat{\varrho}}_i) + \tilde{\theta}_i\Gamma_1^{-1}(\Gamma_1\tau_{i,n} - \dot{\hat{\theta}}_i)) \\ & - \Gamma_2^{-1}\sum_{j\in N_i}\tilde{\theta}_j(\Gamma_2\tau_{j,n} + \dot{\hat{\theta}}_j)] + \Delta \\ = & -\sum_{i=1}^{m}\sum_{k=1}^{n} c_{i,k}z_{i,k}^2 + \Delta\end{aligned} \tag{3.33}$$

where $\Delta = m(\varepsilon_1 + \bar{\epsilon}_i\varepsilon_2 + \frac{\varepsilon_3}{1-\delta} + \frac{\varepsilon_4}{1-\delta})$. Via integration operation, the above inequation can be computed as

$$\begin{aligned}V(t) &\leq V(0) + \Delta - \sum_{i=1}^{m}\sum_{k=1}^{n} c_{i,k}\int_0^T z_{i,k}^2 dt \\ &\leq V(0) + \Delta\end{aligned} \tag{3.34}$$

This implies that $V(0)$ and $V(t)$ are bounded, accompanied by $z_{i,k}, \tilde{\theta}_i, \tilde{\theta}_j, \tilde{\varrho}_i \in L_\infty$. Based on the predefinition, $y_r, \theta_i, \theta_j, \varrho_i$ are ensured bounded, then it is easy to obtain that $x_{i,1}, x_{j,1}, \hat{\theta}_i, \hat{\theta}_j, \hat{\varrho}_i \in L_\infty$. Since the continuous function $\varphi_{i,j}$ and the virtual controller $\alpha_{i,1}$ are bounded defined, $x_{i,2}$ is also bounded. Subsequently, all the variables x_{ij} can be proved bounded and the neighbor control signals $\breve{u}_j$ can be ensured bounded.

Based on the Barbalat's Lemma [28], the consensus tracking errors can be guaranteed to asymptotically converge to zero with the conditions of $z_{i,1}(t) \in \pounds_2$ and $\dot{z}_{i,1}(t) \in \pounds_\infty$, i.e., $\lim_{t\longrightarrow\infty} z_{i,1}(t) = 0$. The bound for the L_2-norm of the tracking error can be expressed as

$$\begin{aligned}\|z_{i,1}(t)\|_{2[0,T]} &= \sqrt{\int_0^T z_{i,1}^2(t)dt} \\ &\leq \frac{1}{\sqrt{2c_{i,1}}}\Big(\underline{\rho}_i\tilde{\varrho}_i^T(0)\Gamma_{\varrho}^{-1}\tilde{\varrho}_i(0) + \tilde{\theta}_i^T(0)\Gamma_1^{-1}\tilde{\theta}_i(0) + \sum_{j\in N_i}\tilde{\theta}_j^T(0)\Gamma_2^{-1}\tilde{\theta}_j(0) \\ &\quad + 2\Delta\Big)^{\frac{1}{2}}\end{aligned} \tag{3.35}$$

The Zeno phenomenon, will lead to physical unrealization, i.e., the preset events may infinitely be triggered in finite time. To prove that the established event-triggered mechanisms are able to avoid this issue, a lower bound of the inter-execution time $t_* > 0$ satisfying the condition of $\{t_{h+1} - t_h\}$ is required. Actually, $e_{t,k}(t) = u_{j,k}(t) - \breve{u}_{j,k}(t), \forall t \in [t_h, t_{h+1})$ is bounded defined, so

$$\frac{d}{dt}|e_t(t)| = sign(e_t)\dot{e}_t \leq |\dot{u}_{j,1}| \tag{3.36}$$

The function $\dot{u}_{i,1}$ contains the variable of $\alpha_{i,1}$, therefore $\dot{u}_{i,1} \in L_2$, i.e., $|\dot{u}_{i,1}| \leq \zeta$, where ζ is a positive constant. Give $e_t(t_h) = 0$, which yields that $\lim_{t\to t_{h+1}} e_t(t) = |\breve{u}_{j,k}(t)| + b$. The following inequation is finally given as

$$\frac{d}{dt}|e_t(t)| = \lim_{t_k\to t_{h+1}}\frac{e_t(t_{h+1}) - e_t(t_h)}{t_{h+1} - t_h} \leq \zeta \tag{3.37}$$

This means that the lower bound of the inter-execution time is successfully found, i.e., $t^* \geq (|\breve{u}_j(t)| + b)/\zeta$. That is to say, all the events can avoid triggering infinite times within a finite time interval.

Remark 3. Most studies on event-triggered strategies sacrifice system performance to increase communication rates. However, based on Theorem 1, it is observed that our method uniquely maintains high communication rates while ensuring stable system performance, accompanied with consensus tracking errors converging to zero asymptotically. Additionally, with the guidance of the established transient performance inequation (3.35), a controlled system can quickly and efficiently adapt to changes.

4. Simulation study

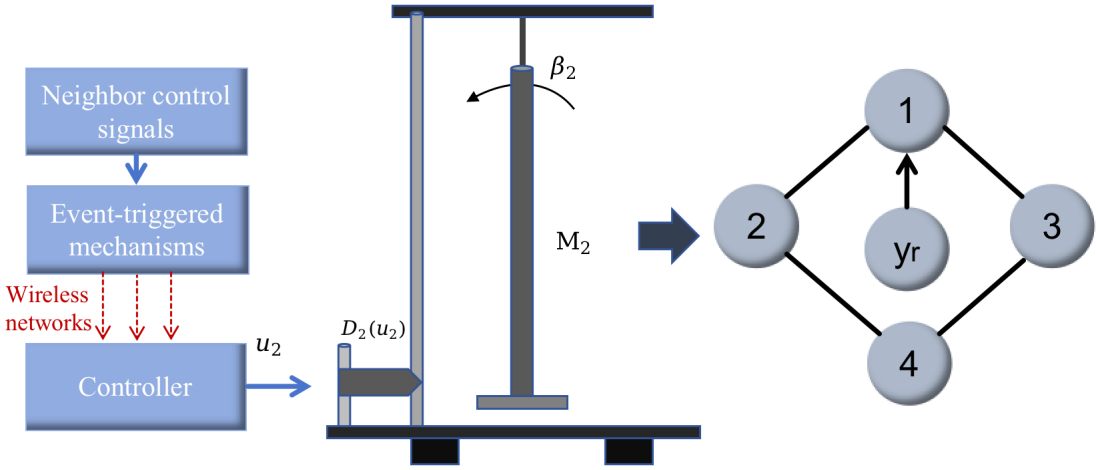

Figure 3. Four continuous torsional pendulum systems.

The section works on verifying feasibility of the proposed method. As discussed in [29], the four continuous torsional pendulum models are employed for our studies, which can be expressed as

$$\begin{aligned} \frac{d\beta_i}{dt} &= \omega_i \\ J_i \frac{d\omega_i}{dt} &= D_i(u_i) - M_i g_i l_i \sin(\beta_i) - f_{d,i} \frac{d\beta_i}{dt} \end{aligned} \tag{4.1}$$

where β_i and ω_i are treated as the angle and angular velocity for ith link, respectively. M_i, l_i and J_i represent the mass, the length and the rotary inertia of ith pendulum, while the coefficients $g_i, f_{d,i}$ are the acceleration of gravity and the frictional factor, respectively. All these parameters are unknown and unavailable. The motor torques of the systems contain dead zone nonlinearity, i.e., $D_i(u_i)$. By giving the definition of $x_{i,1} = \beta_i$ and $x_{i,2} = \omega_i$, one has the following parametric strict-feedback form.

$$\begin{aligned} \dot{x}_{i,1} &= x_{i,2} \\ \dot{x}_{i,2} &= J_i^{-1} D_i(u_i) - [\sin(x_{i,1}), x_{i,2}]\theta_i \end{aligned} \tag{4.2}$$

where $\theta_i = [\frac{M_i g_i l_i}{J_i}, \frac{f_{d,i}}{J_i}]^T$ is remaining to estimate. The physical system model and the communication topology can be graphically represented in Figure 3. From the connection graph of 4 subsystems, the

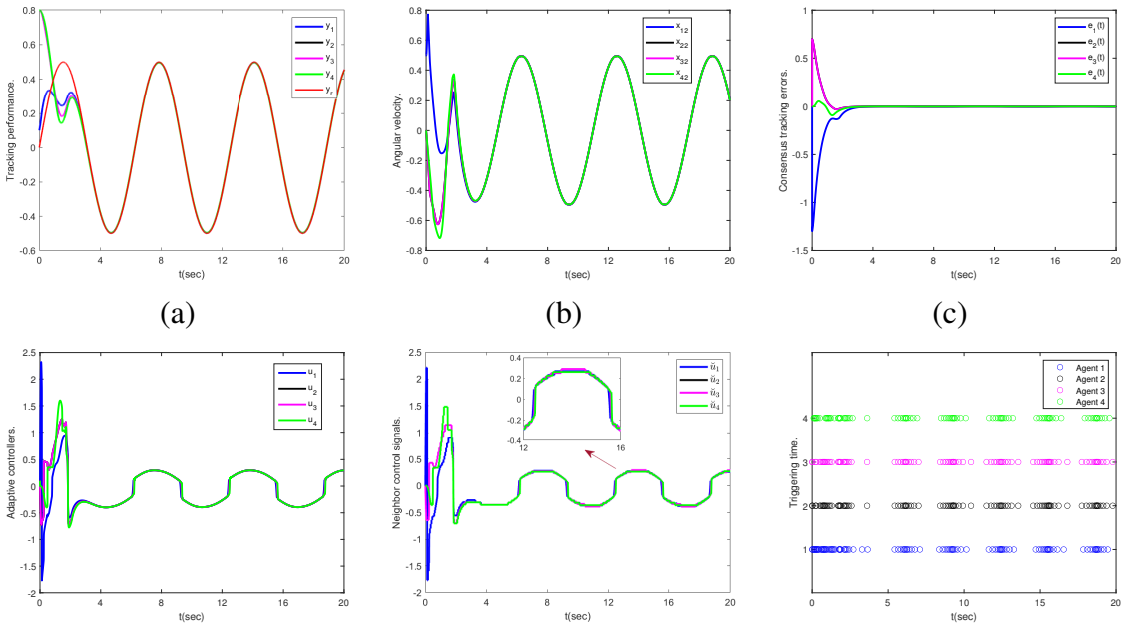

(a) (b) (c)

(d) (e) (f)

Figure 4. The proposed scheme with neighbor event-triggered mechanisms: (a) Tracking performances. (b) Angular velocity x_{i2}. (c) Consensus errors $e_i(t)$. (d) Consensus controllers u_i. (e) Neighbor control signals $\breve{u}_j$. (f) Triggering times of ith agent.

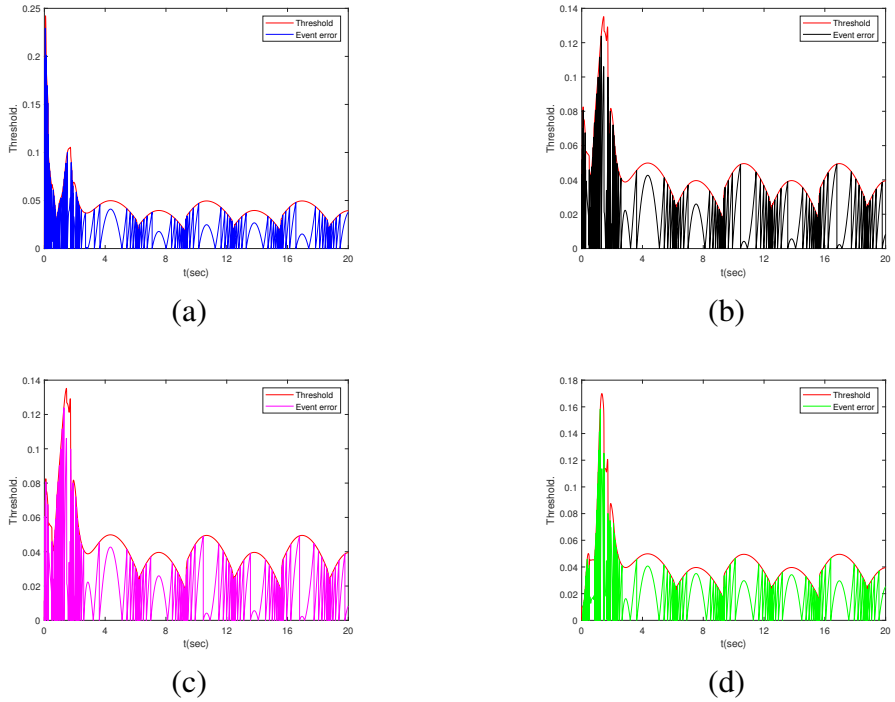

(a) (b)

(c) (d)

Figure 5. The proposed neighbor event-triggered mechanisms with relative thresholds for ith agent, respectively.

values are preset as $b_i = 1$ and $a_{i,j} = 1$ only when two neighbor agents are connected, or $b_i = 0$ and $a_{i,j} = 0$. The leader's signal is set by $y_r = \sin(t)$ and the dead zone parameters are given as $\rho_{i,r} = 2, \rho_{i,l} = 2, b_{ir} = 0.1, b_{il} = -0.2$. The event-triggered neighbor control signals $\breve{u}_j(t)$ are defined as (2.8), where the relative threshold is set as $\delta|u_j(t)| + m_j, \delta = 0.1, m_j = 0.01$. Via the operator of initialization with $x_{1,1}(0) = 0.1, x_{1,2}(0) = 0.5, x_{2,1}(0) = x_{3,1}(0) = x_{4,1}(0) = 0.8, x_{2,2}(0) = x_{3,2}(0) = x_{4,2}(0) = 0, y_r(0) = 0, u_i(0) = 0.1, \hat{\theta}_i(0) = [0, 0]^T, \hat{\varrho}_i(0) = [0, 0, 0, 0]^T$, and the operator of selecting proper user-defined parameters as $c_{i,j} = 2, \Gamma_1 = \Gamma_2 = 5.2, \varepsilon_i = 0.001$, for $i = 1, 2, 3, 4, j = 1, 2$, the simulation results of this method can be seen from Figure 4.

The results presented in Figure 4 illustrate the following points:

- The outputs of all the subagents, represented by y_i, can successfully track the leader's trajectory, denoted as y_r, despite the presence of dead zone nonlinearities in the motor actuators.
- The consensus errors, e_i, are guaranteed to asymptotically converge to zero.
- The neighbor control signals, $\breve{u}_i$, are discretized using the jointly designed event-triggered mechanisms.
- Each of the triggering mechanisms is configured to avoid Zeno behavior.

Additionally, Figure 5 demonstrates the implementation of the neighbor event-triggered mechanisms that utilize relative thresholds.

5. Conclusions

The distributed control problem for multi-agent systems with neighboring communication bandwidth constraints and dead zone inputs is addressed in this paper. The aforementioned bandwidth constraints are managed using the proposed event-triggered mechanisms, which are applicable to the control signals exchanged among neighbors and feature more adaptable relative threshold configurations. Moreover, the decomposition of the dead zone nonlinearity, when coupled with event-triggered coefficients, is effectively neutralized by the specially designed consensus controllers. The proposed methodology ensures closed-loop signal ultimate boundedness for all closed-loop signals, guarantees that consensus errors asymptotically approach zero, and precludes the possibility of Zeno behavior. Simulation results corroborate the effectiveness of our approach.

Use of AI tools declaration

The authors declare they have not used Artificial Intelligence (AI) tools in the creation of this article.

Acknowledgments

This research was funded by the National Natural Science Foundation of China [No.621002153], and the Guangzhou Municipal Science and Technology Project [No.202201010381].

Conflict of interest

The authors declare that they have no conflict of interest.

References

1. R. Postoyan, P. Tabuada, D. Nesic, A. Anta, A framework for the event-triggered stabilization of nonlinear systems, *IEEE T. AUTOMAT. CONTR.*, **60** (2015), 982–996. https://doi.org/10.1109/TAC.2014.2363603
2. S. Liu, B. Niu, G. Zong, X. Zhao, N. Xu, Data-driven-based event-triggered optimal control of unknown nonlinear systems with input constraints, *NONLINEAR DYNAM.*, **109** (2022), 891–909. https://doi.org/10.1007/s11071-022-07459-7
3. X. Han, X. Zhao, T. Sun, Y. Wu, N. Xu, G. Zong, Event-triggered optimal control for discrete-time switched nonlinear systems with constrained control input, *IEEE T. SYST. MAN CY.-S.*, **51** (2021), 7850–7859. https://doi.org/10.1109/TSMC.2020.2987136
4. L. Xing, C. Wen, Z. Liu, H. Su, J. Cai, Adaptive compensation for actuator failures with event-triggered input, *AUTOMATICA*, **85** (2017), 129–136. https://doi.org/10.1016/j.automatica.2017.07.061
5. J. Zhang, D. Yang, H. Zhang, Y. Wang, B. Zhou, Dynamic event-based tracking control of boiler turbine systems with guaranteed performance, *IEEE T. AUTOM. SCI. ENG.*, (2023), to be published. https://doi.org/10.1109/TASE.2023.3294187
6. L. Cao, H. Li, G. Dong, R. Lu, Event-triggered control for multiagent systems with sensor faults and input saturation, *IEEE T. SYST. MAN CY.-S.*, **51** (2021), 3855–3866. https://doi.org/10.1109/TSMC.2019.2938216
7. J. Huang, W. Wang, C. Wen, G. Li, Adaptive event-triggered control of nonlinear systems with controller and parameter estimator triggering, *IEEE T. AUTOMAT. CONTR.*, **65** (2020), 318–324. https://doi.org/10.1109/TAC.2019.2912517
8. H. Wang, K. Xu, J. Qiu, Event-triggered adaptive fuzzy fixed-time tracking control for a class of nonstrict-feedback nonlinear systems, *IEEE T. CIRCUITS-I*, **68** (2021), 3058–3068. https://doi.org/10.1109/TCSI.2021.3073024
9. J. Zhang, H. Zhang, S. Sun, Y. Cai, Adaptive time-varying formation tracking control for multiagent systems with nonzero leader input by intermittent communications, *IEEE T. CYBERNETICS*, **53** (2023), 5706–5715. https://doi.org/10.1109/TCYB.2022.3165212
10. X. Li, Z. Sun, Y. Tang, H. R. Karimi, Adaptive event-triggered consensus of multiagent systems on directed graphs, *IEEE T. AUTOMAT. CONTR.*, **66** (2021), 1670–1685. https://doi.org/10.1109/TAC.2020.3000819
11. W. Hu, C. Yang, T. Huang, W. Gui, A distributed dynamic event-triggered control approach to consensus of linear multiagent systems with directed networks, *IEEE T. CYBERNETICS*, **50** (2020), 869–874. https://doi.org/10.1109/TCYB.2018.2868778
12. H. Zhang, J. Zhang, Y. Cai, S. Sun, J. Sun, Leader-following consensus for a class of nonlinear multiagent systems under event-triggered and edge-event triggered mechanisms, *IEEE T. CYBERNETICS*, **52** (2022), 7643–7654. https://doi.org/10.1109/TCYB.2020.3035907
13. Q. Zhou, W. Wang, H. Ma, H. Li, Event-triggered fuzzy adaptive containment control for nonlinear multiagent systems with unknown bouc-wen hysteresis input, *IEEE T. FUZZY SYST.*, **29** (2021), 731–741. https://doi.org/10.1109/TFUZZ.2019.2961642

14. Y. Wang, Z. Chen, M. Sun, Q. Sun, A novel implementation of an uncertain dead-zone-input-equipped extended state observer and sign estimator, *INFORM. SCIENCES*, **626** (2023), 75–93. https://doi.org/10.1016/j.ins.2023.01.060

15. Z. Zhao, Z. Tan, Z. Liu, M. O. Efe, C. K. Ahn, Adaptive inverse compensation fault-tolerant control for a flexible manipulator with unknown dead-zone and actuator faults, *IEEE T. IND. ELECTRON.*, **70** (2023), 12698–12707. https://doi.org/10.1109/TIE.2023.3239926

16. Z. Xi, Y. Wang, H. Zhang, F. Sun, Q. Zheng, Z. Zhu, Research on afterburning control of more electric engine with a nonlinear fuel supply system, *PROCEEDINGS OF THE INSTITUTION OF MECHANICAL ENGINEERS PART G-JOURNAL OF AEROSPACE ENGINEERING*, **237** (2023), 2647–2664. https://doi.org/10.1177/09544100231155696

17. Z. Wang, X. Wang, Fault-tolerant control for nonlinear systems with a dead zone: Reinforcement learning approach, *MATH. BIOSCI. ENG.*, **20** (2023), 6334–6357. https://doi.org/10.3934/mbe.2023274

18. V.-T. Nguyen, T.-T. Bui, H.-Y. Pham, A finite-time adaptive fault tolerant control method for a robotic manipulator in task-space with dead zone, and actuator faults, *INT. J. CONTROL AUTOM. SYST.*, (2023), to be published. https://doi.org/10.1007/s12555-022-1069-5

19. S. Dong, Y. Zhang, Identification modelling and fault-tolerant predictive control for industrial input nonlinear actuator system, *MACHINES*, **11** (2023), 240. https://doi.org/10.3390/machines11020240

20. Y. H. Pham, T. L. Nguyen, T. T. Bui, T. Nguyen, V, Adaptive active fault tolerant control for a wheeled mobile robot under actuator fault and dead zone, *IFAC PAPERSONLINE*, **55** (2022), 314–319. https://doi.org/10.1016/j.ifacol.2022.11.203

21. G. Shao, X.-F. Wang, R. Wang, A distributed strategy for games in euler-lagrange systems with actuator dead zone, *NEUROCOMPUTING*, (2023), to be published. https://doi.org/10.1016/j.neucom.2023.126844

22. W. Wang, T. Wen, X. He, G. Xu, Path following with prescribed performance for under-actuated autonomous underwater vehicles subjects to unknown actuator dead-zone, *IEEE T. INTELL. TRANSP. SYST.*, **24** (2023), 6257–6267. https://doi.org/10.1109/TITS.2023.3248153

23. Z. Liu, F. Wang, Y. Zhang, X. Chen, C. L. P. Chen, Adaptive tracking control for a class of nonlinear systems with a fuzzy dead-zone input, *IEEE T. FUZZY SYST.*, **23** (2015), 193–204. https://doi.org/10.1109/TFUZZ.2014.2310491

24. T. Zhang, R. Bai, Y. Li, Practically predefined-time adaptive fuzzy quantized control for nonlinear stochastic systems with actuator dead zone, *IEEE T. FUZZY SYST.*, **31** (2023), 1240–1253. https://doi.org/10.1109/TFUZZ.2022.3197970

25. J. Wang, Y. Yan, J. Liu, C. L. P. Chen, Z. Liu, C. Zhang, Nn event-triggered finite-time consensus control for uncertain nonlinear multi-agent systems with dead-zone input and actuator failures, *ISA T.*, **137** (2023), 59–73. https://doi.org/10.1016/j.isatra.2023.01.032

26. Y. Wang, B. Ma, D. Wang, T. Chai, Event-triggered prespecified performance control for steer-by-wire systems with input nonlinearity, *IEEE T. INTELL. TRANSP. SYST.*, **24** (2023), 6922–6931. https://doi.org/10.1109/TITS.2023.3242949

27. L. Xing, C. Wen, Z. Liu, H. Su, J. Cai, Event-triggered output feedback control for a class of uncertain nonlinear systems, *IEEE T. AUTOMAT. CONTR.*, **64** (2019), 290–297. https://doi.org/10.1109/TAC.2018.2823386

28. A. Souahi, O. Naifar, A. Ben Makhlouf, M. A. Hammami, Discussion on barbalat lemma extensions for conformable fractional integrals, *INT. J. CONTROL*, **92** (2019), 234–241. https://doi.org/10.1080/00207179.2017.1350754

29. Y.-X. Li, G.-H. Yang, S. Tong, Fuzzy adaptive distributed event-triggered consensus control of uncertain nonlinear multiagent systems, *IEEE T. SYST. MAN CY.-S.*, **49** (2019), 1777–1786. https://doi.org/10.1109/TSMC.2018.2812216

AIMS Press